

## Table of Contents

Description of the Finite Element Model Setup .....	2
1.1 Geometry of the Plate.....	2
1.2 Boundary Conditions.....	2
1.3 Element Type .....	3
Element Family and Element Shape .....	3
Assigning Element Type .....	3
Plane Stress / Plane Strain .....	3
Material Properties .....	4
1.4 Mesh Configuration and Mesh Convergence .....	4
Mesh Technique.....	4
Convergence Analysis .....	5
Seed and Mesh Control.....	5
Post-Processing and Examination of Results .....	5
2.1 Theoretical calculation of the stress field around the hole .....	5
Kirsch's Solution .....	5
Superposition .....	7
2.2 Distribution of the stress field from FE analysis .....	8
2.3 Plots of stress ratios.....	10
$\theta = 0$ .....	10
$\theta = \pi/4$ .....	12
$\theta = \pi/2$ .....	13
3 Discussion.....	14
3.1 Location and magnitude of maximum stress concentration factor (SCF) .....	14
Stress concentration factor.....	15
Theoretical Prediction of S.....	15
FE Analysis of S.....	15
Reasons for Discrepancies .....	18
3.2 Effect of Plate Dimension on Stress Concentration Factor .....	19
References .....	20

# Description of the Finite Element Model Setup

## 1.1 Geometry of the Plate

The model of a quarter part of the plate is shown in figure 1, with dimensions labelled in meters.

Steps:

1. Module: Part
2. 2D planar space
3. Draw a square and a circle as the plate and the hole
4. Auto-trim excessive lines

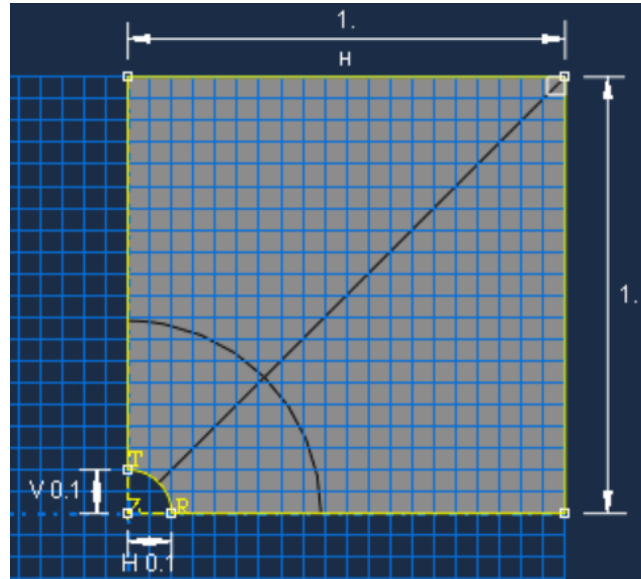


Figure 1: Plate dimension

## 1.2 Boundary Conditions

There are two boundary conditions imposed into this model, the bottom boundary condition symmetrical along the y-axis and the left boundary condition symmetrical along the x-axis. This is shown through the orange triangles shown in figure 2.

Steps:

1. Module: Load
2. Click on “create boundary condition”
3. Select mechanical and symmetry as the category
4. Select the bottom and the left sets to assign a boundary condition for both individually

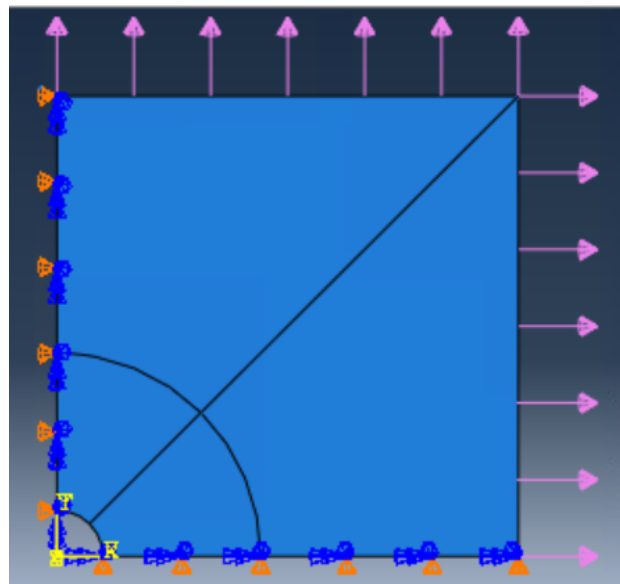


Figure 2: Boundary condition and loads of plate

The author's first name begins with C, hence the stress biaxiality ratio used is  $\frac{\sigma_1}{\sigma_2} = 4.5$ .

Therefore, the stresses applied are  $\sigma_1 = 4500 \text{ Pa}$  and  $\sigma_2 = 1000 \text{ Pa}$ .

### 1.3 Element Type

#### Element Family and Element Shape

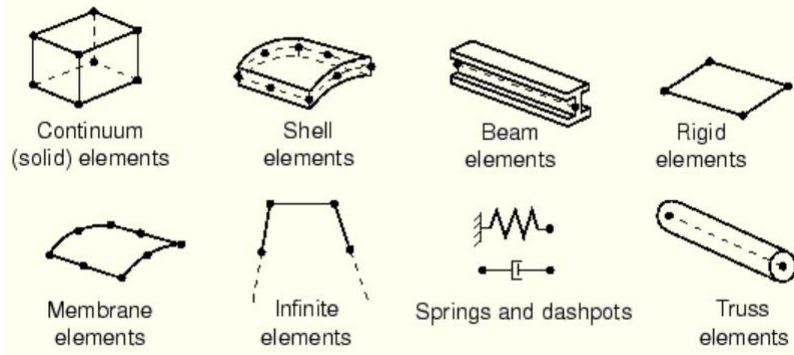


Figure 3: Common element families

Figure 3 shows eight of the common element family in stress analysis. [1]

There consists of three element shapes (quadrilateral, quad-dominant and triangular) in 2D analysis.

First-order triangular elements are avoided in stress analysis situations as the elements produced will be stiff and show slow convergence with mesh refinement. The mesh density that would be used in ABAQUS is rather high, hence finer mesh should be used for more accurate results and triangular elements will not be used. Similarly, quad-dominant elements are not suitable as they are normally used for incompressible materials.

Additionally, continuum element best describes single homogeneous material, which is aluminium in this scenario, typically used for stress analysis. Quadrilateral and hexahedra (for 3D) elements are normally used with continuum element. Therefore, quadrilateral element is chosen.

#### Assigning Element Type

Steps:

1. Module: Mesh
2. Assign element type
3. “Standard” and “Linear” are the defaults used in element library and geometric order selection

#### Plane Stress / Plane Strain

Plane stress elements are used to model thick structures, assuming the plane strain in the z direction is zero,  $\varepsilon_{zz} = 0$ . On the other hand, plane strain elements are used to model thin

structures, assuming the plane stress in the z direction is zero,  $\sigma_{zz} = 0$ . Therefore, plane strain is chosen for this thin plate. [1]

### Material Properties

Aluminium is used in this analysis with a Young's modulus of  $E = 70 \times 10^9 \text{ Pa}$  and Poisson ratio of  $\nu = 0.33$ .

Steps:

1. Module: Property
2. Create material
3. Under mechanical, select "elasticity" then "elastic"
4. Choose the type as "isotropic" and input Young's modulus and Poisson's ratio

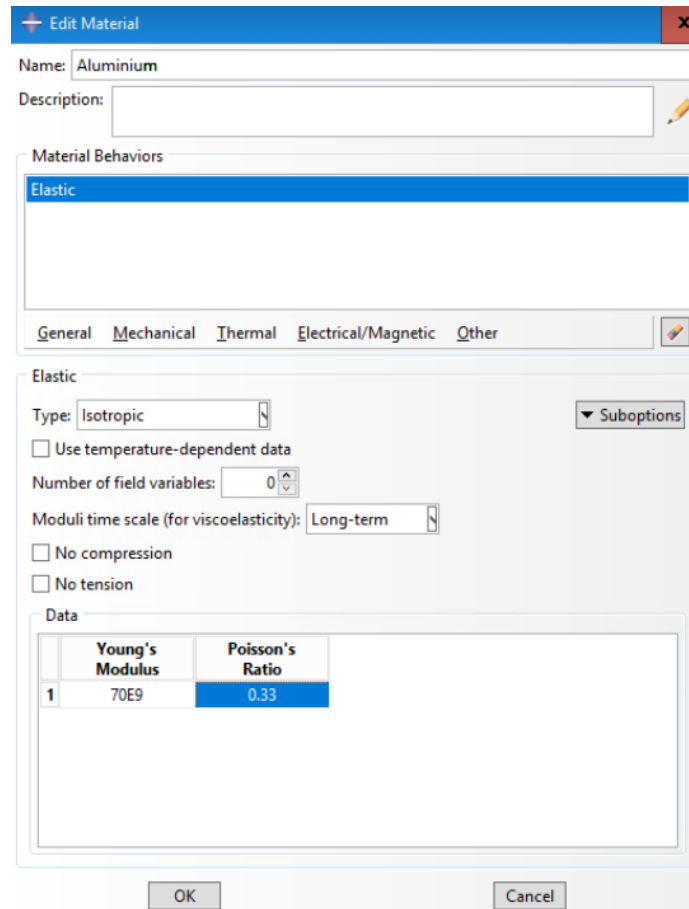


Figure 4: Material of plate

### 1.4 Mesh Configuration and Mesh Convergence

#### Mesh Technique

Structured mesh is chosen as it gives the most control over the mesh as it applies pre-established mesh patterns to particular model topologies.

The ideology of a good mesh is defined through the following points:

1. Finer mesh in high stress regions
2. No dramatic changes in mesh size and shape

Through the criteria above, free mesh is not suitable as there are irregular distribution of elements. Structured mesh gives organised and uniform transition of element size. [2]

## Convergence Analysis

Using S22 to perform this analysis, as it has the largest maximum stress amongst the three stress distribution graphs.

Abaqus can only simulate up to 250000 nodes, each quad element has 4 nodes.

Seed Size	Element Number	Maximum Stress	Convergence
0.002	242990	1.256E+04	-
0.004	60138	1.231E+04	-1.99%
0.008	14835	1.187E+04	-3.57%
0.016	3528	1.110E+04	-6.49%
0.032	868	1.010E+04	-9.01%
0.064	180	8.612E+03	-14.73%
0.128	64	7.544E+03	-12.40%

Table 1: Convergence

The convergence chosen is  $\pm 5\%$ ; therefore, a seed size of 0.008 is used.

## Seed and Mesh Control

Seeds control the distance between elements. Global seeds are used instead of local seeds for the simplicity of the mesh generation.

Steps:

1. Module: Mesh
2. Click “seed part”
3. Assign global seed of 0.008
4. Click assign mesh controls
5. Select “quad” for element shape as explained above
6. Select “structured” technique
7. Click “mesh part” to see mesh

Local seeds can be used to increase the simulation speed by reducing the number of seeds. This lowers the mesh density in regions with lower stress, hence increasing the efficiency of obtaining results without any variations in the data.

## Post-Processing and Examination of Results

### 2.1 Theoretical calculation of the stress field around the hole

#### Kirsch's Solution

Assumptions:

- The plate is thin, hence analysed in a 2D plane
- Uniform stress distribution along all sides of the plate

Using the principle of superposition, the horizontal and vertical components are analysed separately.

The stress field around a hole in an infinite elastic plane can be written as equations in the coordinate system  $(r, \theta)$  as shown below. This is known as the Kirsch's Solution.

$$\sigma_{rr} = \frac{1}{2}\sigma\left(1 - \frac{a^2}{r^2}\right) + \frac{1}{2}\sigma\left(1 - 4\frac{a^2}{r^2} + 3\frac{a^4}{r^4}\right)\cos 2\theta \quad [Eq 1]$$

$$\sigma_{\theta\theta} = \frac{1}{2}\sigma\left(1 + \frac{a^2}{r^2}\right) - \frac{1}{2}\sigma\left(1 + 3\frac{a^4}{r^4}\right)\cos 2\theta \quad [Eq 2]$$

$$\tau_{r\theta} = -\frac{1}{2}\sigma\left(1 + 2\frac{a^2}{r^2} - 3\frac{a^4}{r^4}\right)\sin 2\theta \quad [Eq 3]$$

Pure shear stress occurs when  $\sigma_1 = -\sigma_2$ . Biaxial tension is analysed here, hence  $\tau_{xy}$  is neglected during calculation.

## Superposition

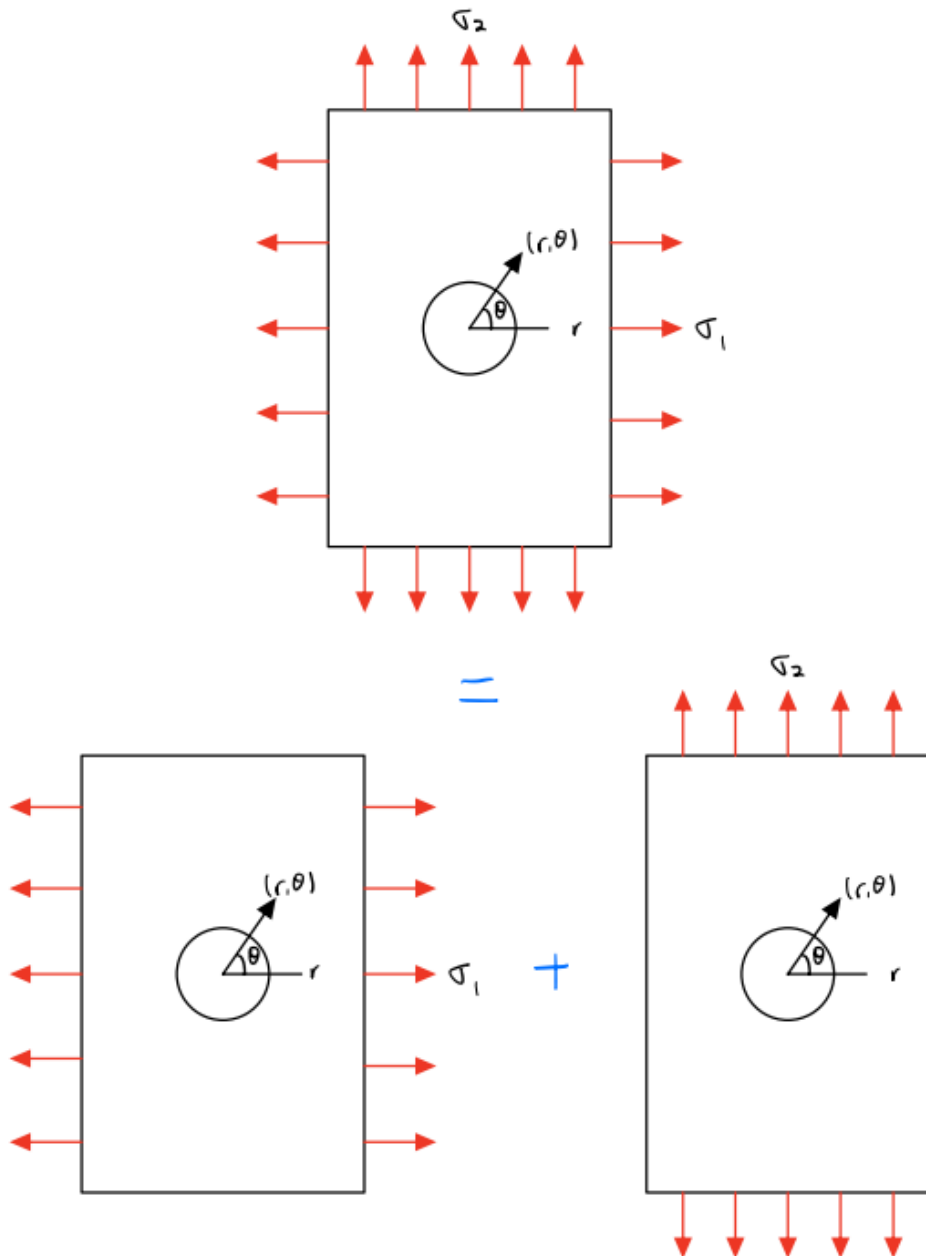


Figure 5: Superposition

Figure 5 illustrates the principle of superposition. The horizontal components are reflected as  $\theta$  and the vertical components can be correlated through  $\theta + \frac{\pi}{2}$ .

$$\sigma_{rr} = \frac{1}{2}(\sigma_2 + \sigma_1)\left(1 - \frac{a^2}{r^2}\right) + \frac{1}{2}(\sigma_2 - \sigma_1)\left(1 - 4\frac{a^2}{r^2} + 3\frac{a^4}{r^4}\right)\cos 2\theta \quad [Eq 4]$$

$$\sigma_{\theta\theta} = \frac{1}{2}(\sigma_2 + \sigma_1)\left(1 + \frac{a^2}{r^2}\right) - \frac{1}{2}(\sigma_2 - \sigma_1)\left(1 + 3\frac{a^4}{r^4}\right)\cos 2\theta \quad [Eq 5]$$

$$\tau_{r\theta} = -\frac{1}{2}(\sigma_2 - \sigma_1)\left(1 + 2\frac{a^2}{r^2} - 3\frac{a^4}{r^4}\right)\sin 2\theta \quad [Eq 6]$$

## 2.2 Distribution of the stress field from FE analysis

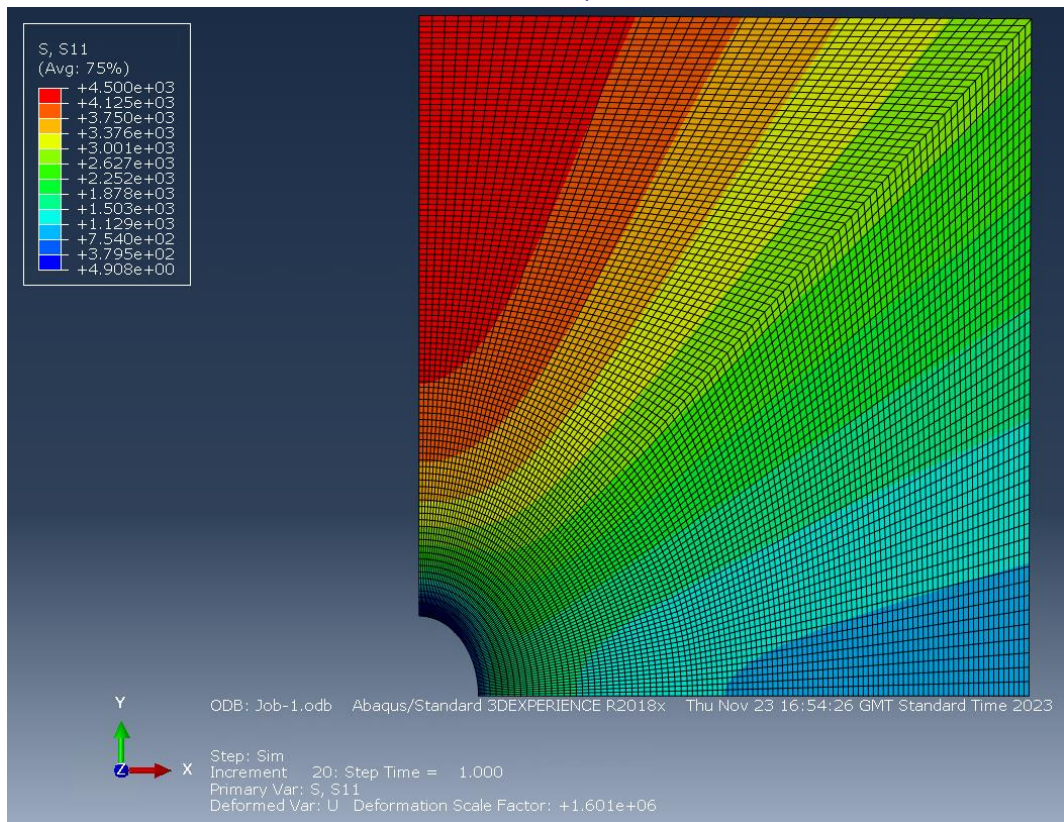


Figure 6:  $S_{11}$  from FE analysis

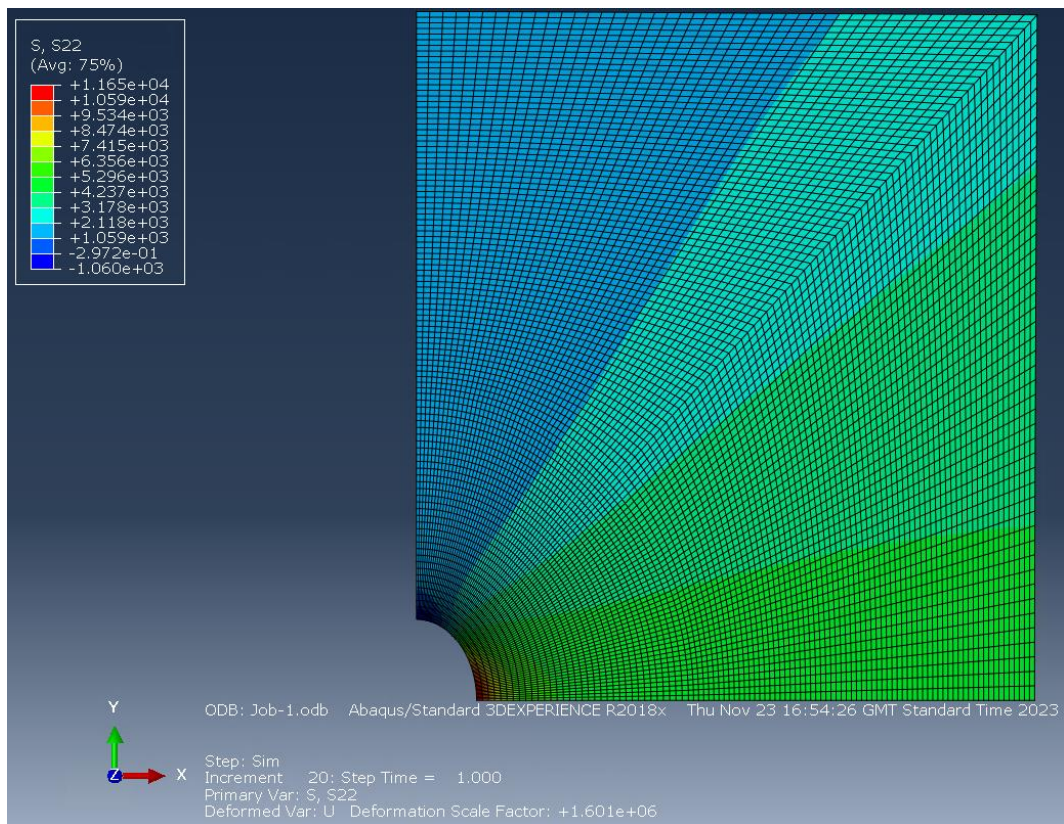


Figure 7: S22 from FE analysis

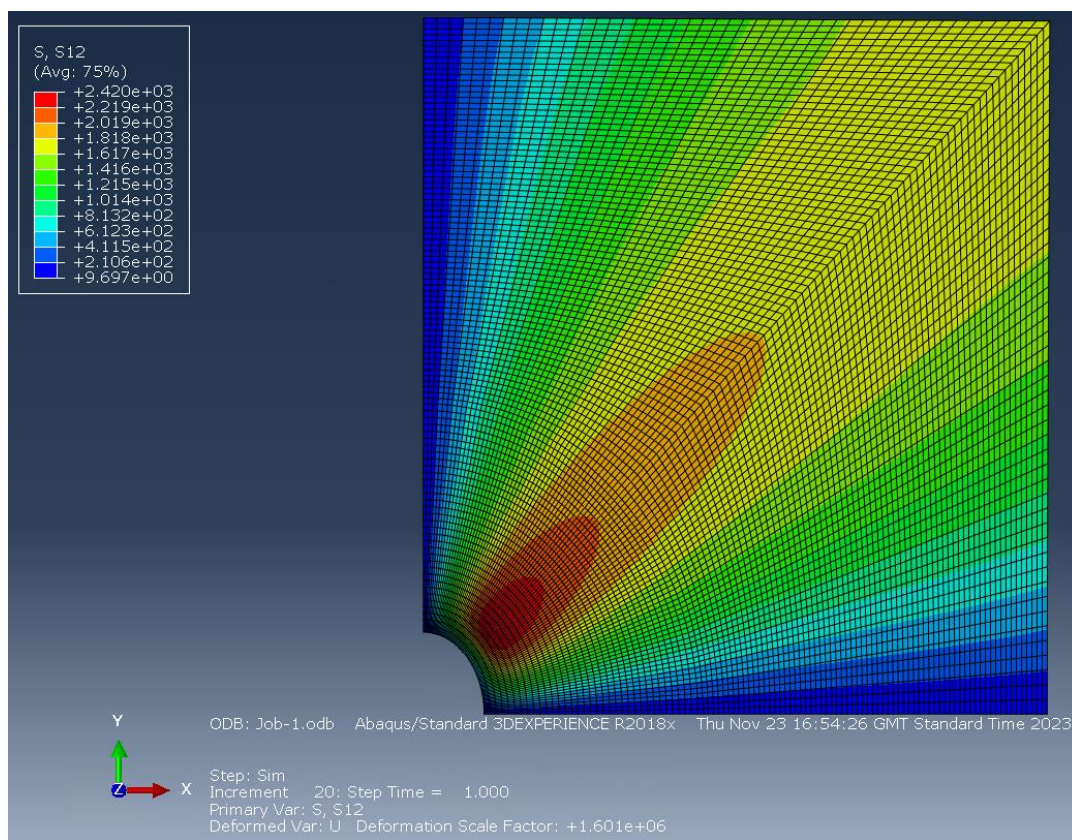


Figure 8: S12 from FE analysis

Figures 6-8 show the distribution of the three stress field components of  $S_{11}$ ,  $S_{22}$  and shear stress  $S_{12}$  respectively.

### 2.3 Plots of stress ratios

The maximum stress is  $\sigma_{max}^{\infty} = \sigma_1 = 4500 \text{ Pa}$  as  $\sigma_1 > \sigma_2$ .

$\tau_{xy} = \tau_{yx}$  in simulation as each element in mesh is infinitesimal.

$S_{11}$ ,  $S_{22}$  and  $S_{12}$  can be related to the stresses as described below.

$$\sigma_{rr} = S_{11}$$

$$\sigma_{\theta\theta} = S_{22}$$

$$\tau_{r\theta} = S_{12}$$

The above relationship is true as the datum coordinate system selected is cylindrical. [3]

$\theta = 0$

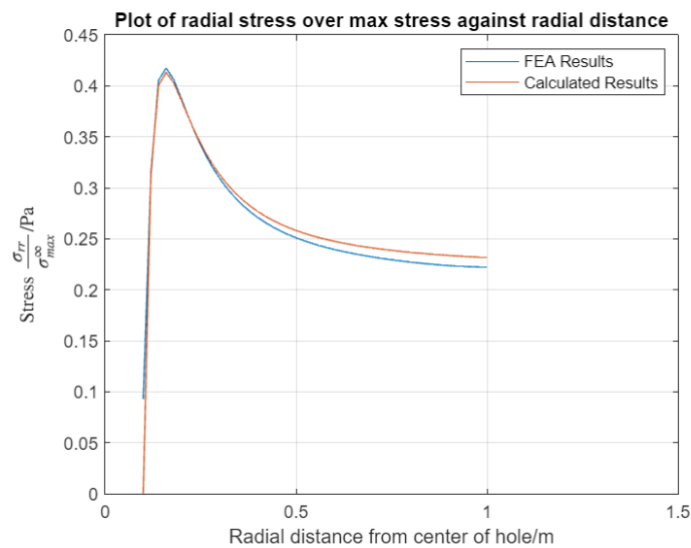


Figure 9: Plot of radial stress over max stress against radial distance at  $\theta = 0$

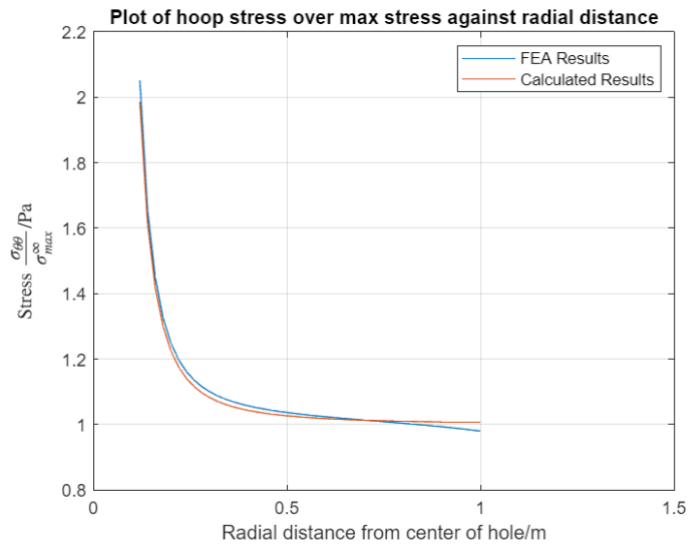


Figure 10: Plot of hoop stress over max stress against radial distance at  $\theta = 0$

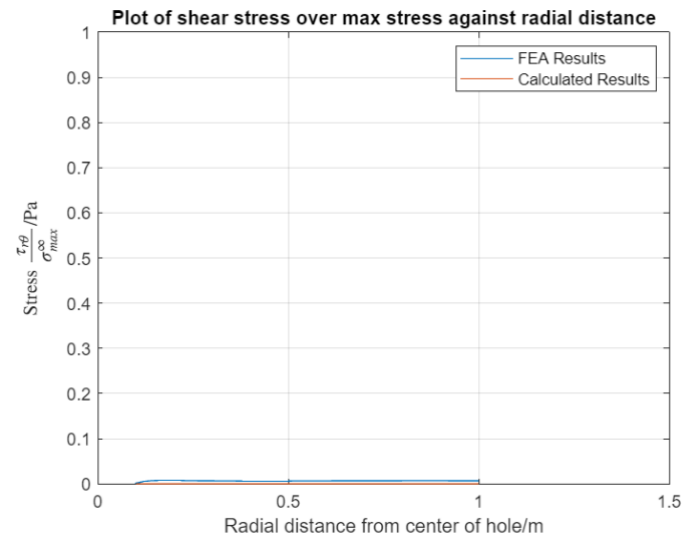


Figure 11: Plot of shear stress over max stress against radial distance at  $\theta = 0$

$$\theta = \frac{\pi}{4}$$

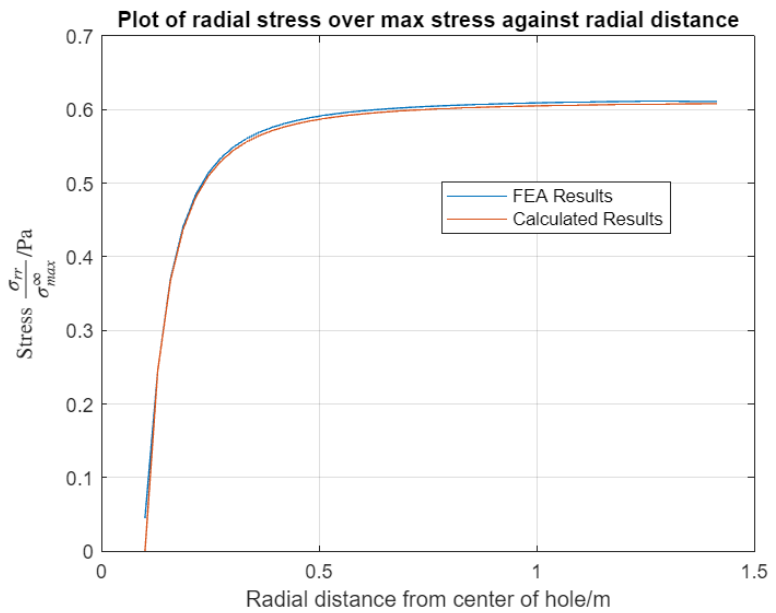


Figure 12: Plot of radial stress over max stress against radial distance at  $\theta = \frac{\pi}{4}$

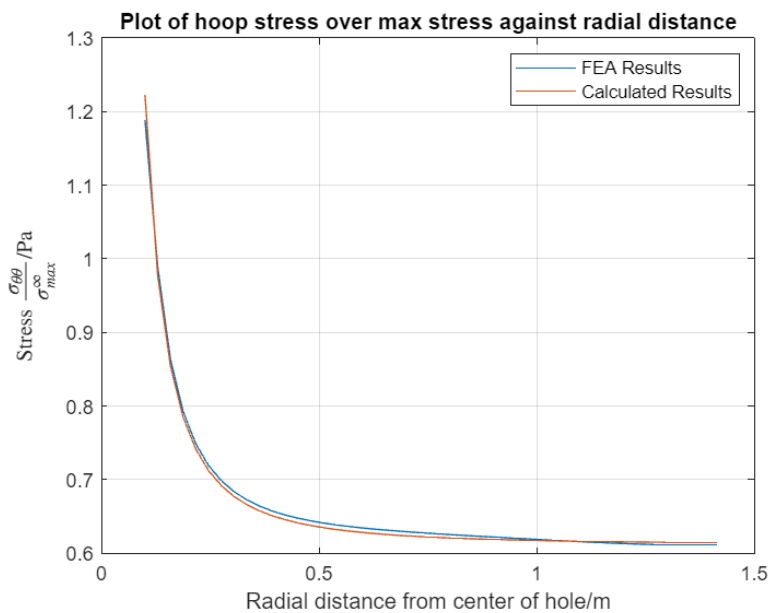


Figure 13: Plot of hoop stress over max stress against radial distance at  $\theta = \frac{\pi}{4}$

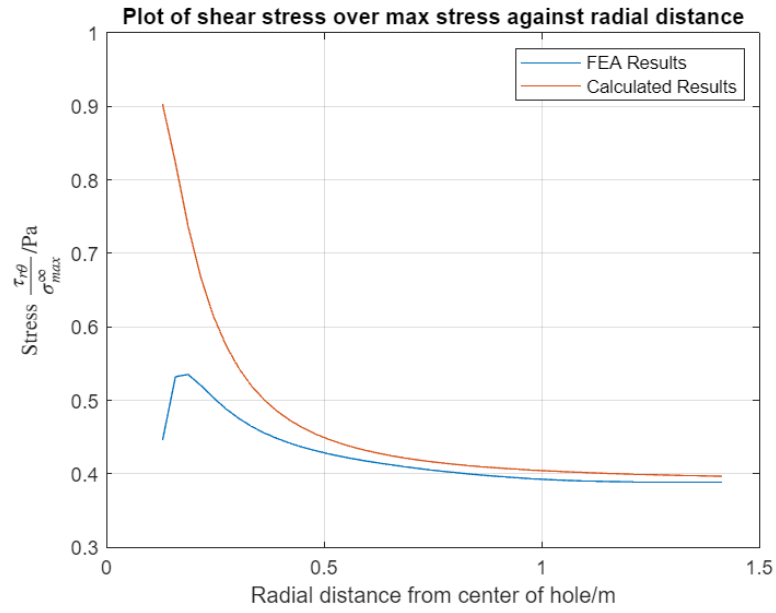


Figure 14: Plot of shear stress over max stress against radial distance at  $\theta = \frac{\pi}{4}$

$$\theta = \frac{\pi}{2}$$

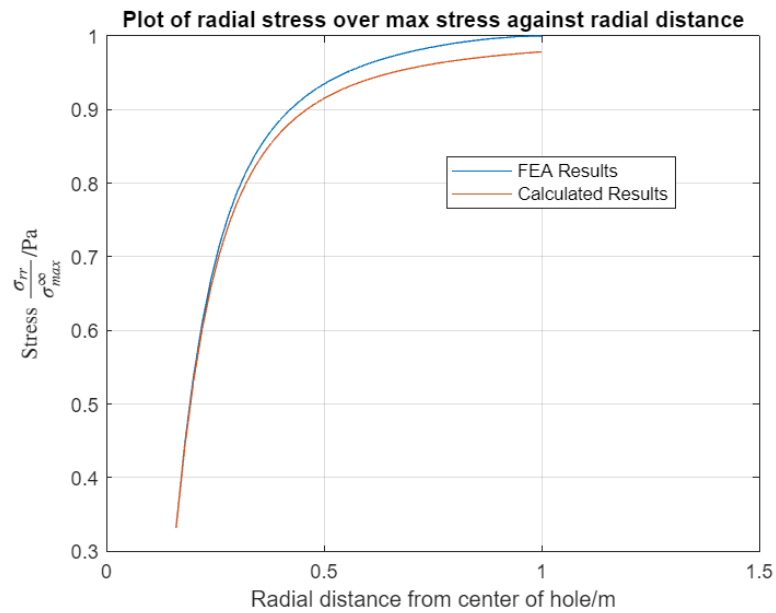


Figure 15: Plot of radial stress over max stress against radial distance at  $\theta = \frac{\pi}{2}$

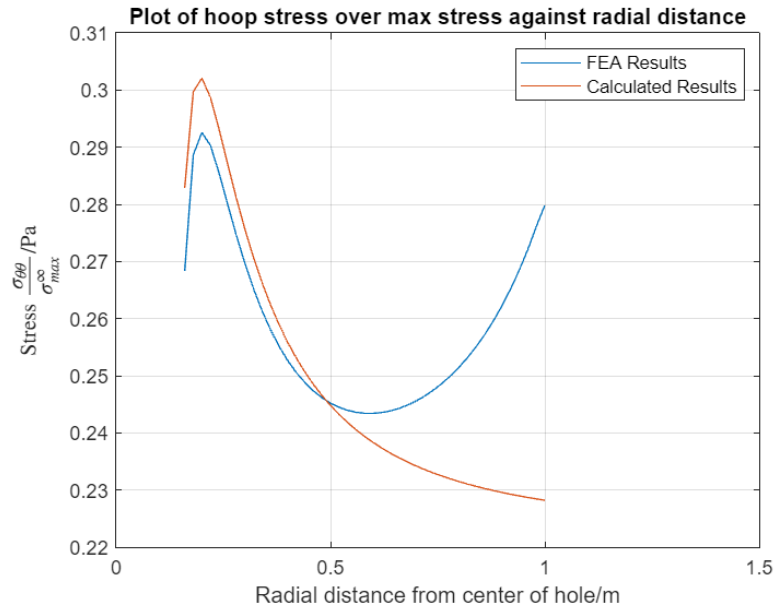


Figure 16: Plot of hoop stress over max stress against radial distance at  $\theta = \frac{\pi}{2}$

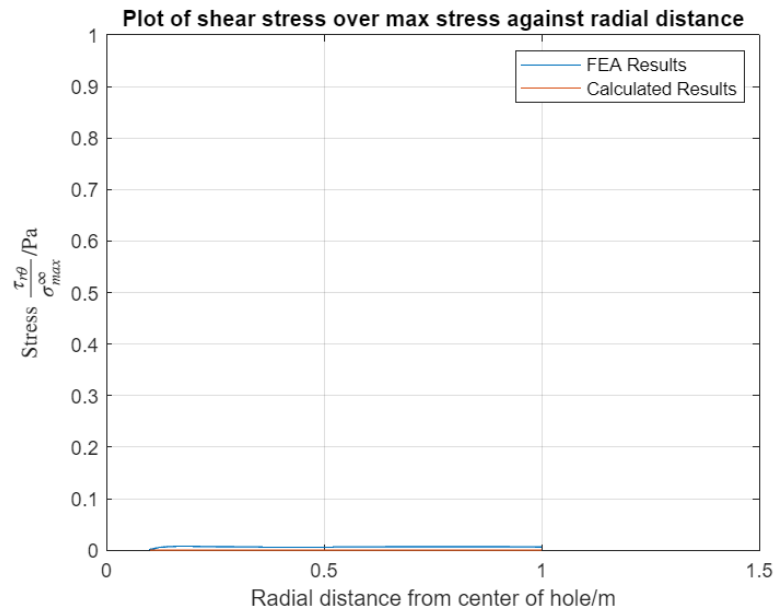


Figure 17: Plot of shear stress over max stress against radial distance at  $\theta = \frac{\pi}{2}$

The data obtained from the ABAQUS path is adjusted by a margin of 0.1m to give radial distance from the center of the hole.

### 3 Discussion

#### 3.1 Location and magnitude of maximum stress concentration factor (SCF)

Stress concentration factor

$$S = \frac{\sigma_{max}^{hole}}{\sigma_{max}^{\infty}} \quad [Eq 7]$$

Theoretical Prediction of S

Using the boundary condition of  $r = a$  at the hole vicinity, equations 4-6 can be written as:

$$\sigma_{rr} = 0$$

$$\sigma_{\theta\theta} = (\sigma_1 + \sigma_2) + 2(\sigma_1 - \sigma_2) \cos 2\theta$$

$$\tau_{r\theta} = 0$$

```
a = 0.1; % Radius of hole is 0.1 m
sigma_1 = 4500; % Vertical tensile stress is 1000 Pa
sigma_2 = 1000; % Horizontal tensile stress is 222.22 Pa
theta = linspace(0,2*pi,100);
hoop_stress = (sigma_1 + sigma_2) + 2*(sigma_1 - sigma_2)*cos(2*theta);
radial_stress = 0*theta;
shear_stress = 0*theta;

plot(theta,hoop_stress,'Color','blue')
hold on
plot(theta,shear_stress,'Color','cyan')
hold on
plot(theta,radial_stress,'Color','red')
xlim([0 2*pi])
hold off

xlabel('(\theta)');
ylabel('Stress (Pa)')
title('Stress on Hole along (\theta)')
legend('(\sigma_{rr})','(\sigma_{\theta\theta})','(\tau_{r\theta})')
grid on
```

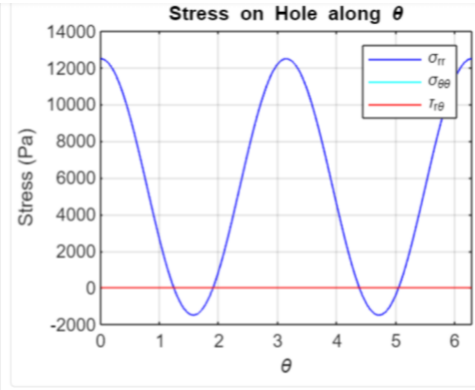


Figure 18: Theoretical prediction of S

Figure 18 shows the change in the magnitude and direction of stress at  $r = a$  along  $\theta$ . The red line illustrates the radial and shear stress, whilst the blue line denotes the hoop stress. The hoop stress witnesses a sinusoidal variation with maximum at 12500 Pa and minimum at -1500 Pa.

$\sigma_{\theta\theta}$  is the largest at  $0, \pi$  and  $2\pi$ , which represents  $\sigma_{max}^{hole}$ .

$$\sigma_{max}^{hole} = \sigma_{\theta\theta} = (\sigma_1 + \sigma_2) + 2(\sigma_1 - \sigma_2) \cos(2 \times \pi) = 12500 \text{ Pa}$$

$$S = \frac{12500}{4500} = 2.78$$

Stress concentrations arises from sudden changes in geometry, sharp radius or edge. When radius of curvature approaches zero, stress concentration factor (SCF) approaches infinity. Conversely, a rise in the radius of curvature reduces the SCF.

FE Analysis of S

S11

```

dataTable = S11Hole;
columnHeaders = {'X', 'S11Hole'};
columnA = dataTable.(columnHeaders{1});
columnB = dataTable.(columnHeaders{2});
sigma_1 = 4500;
sigma_2 = 1000;
a = 0.1;
c = columnA; % Arc length of 0 to pi
plot(c, columnB ./ (sigma_1));

title('SCF along Arc Length');
xlabel('Arc Length');
ylabel('SCF');
grid on

```

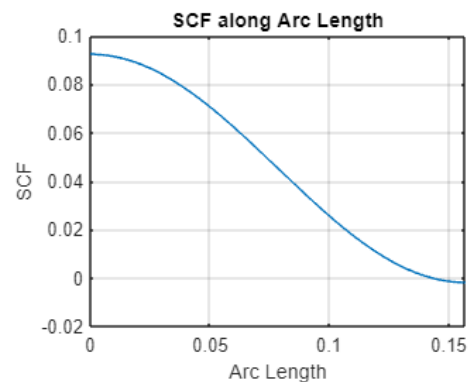


Figure 19: S11 along arc length

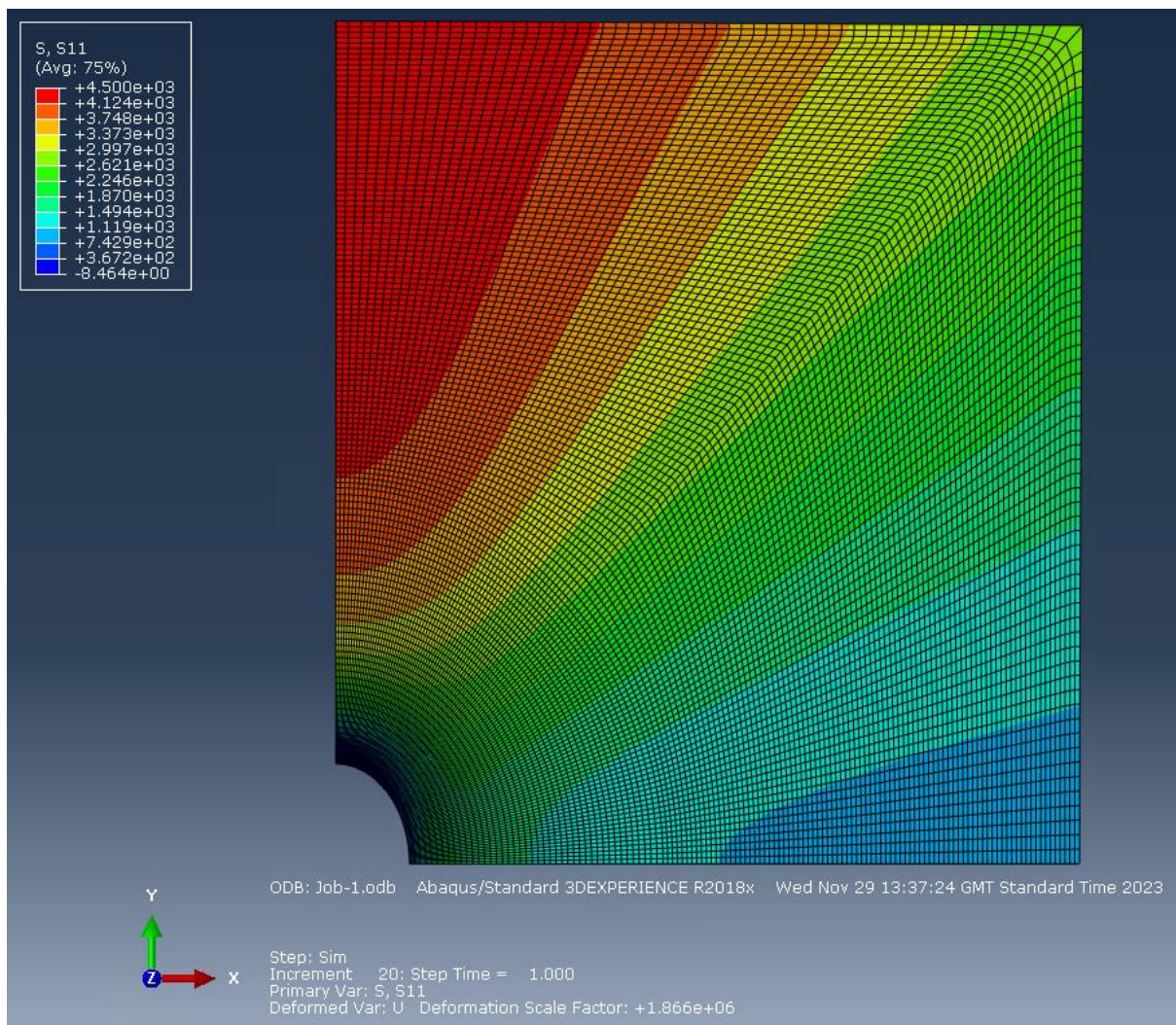


Figure 20: FEA of S11 along arc length

```

dataTable = S22Hole;
columnHeaders = {'X','S22Hole'};
columnA = dataTable.(columnHeaders{1});
columnB = dataTable.(columnHeaders{2});
sigma_1 = 4500;
sigma_2 = 1000;
a = 0.1;
c = columnA; % Arc length of 0 to pi
plot(c,columnB ./ (sigma_1));

title('SCF along Arc Length');
xlabel('Arc Length');
ylabel('SCF');
grid on

```

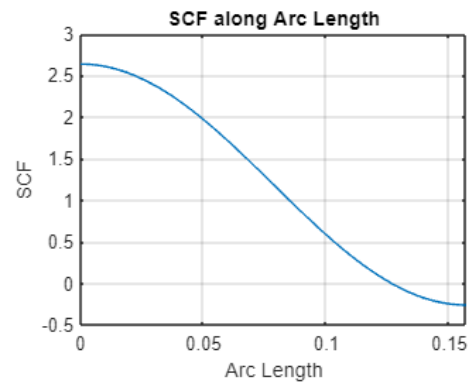


Figure 21: S22 along arc length

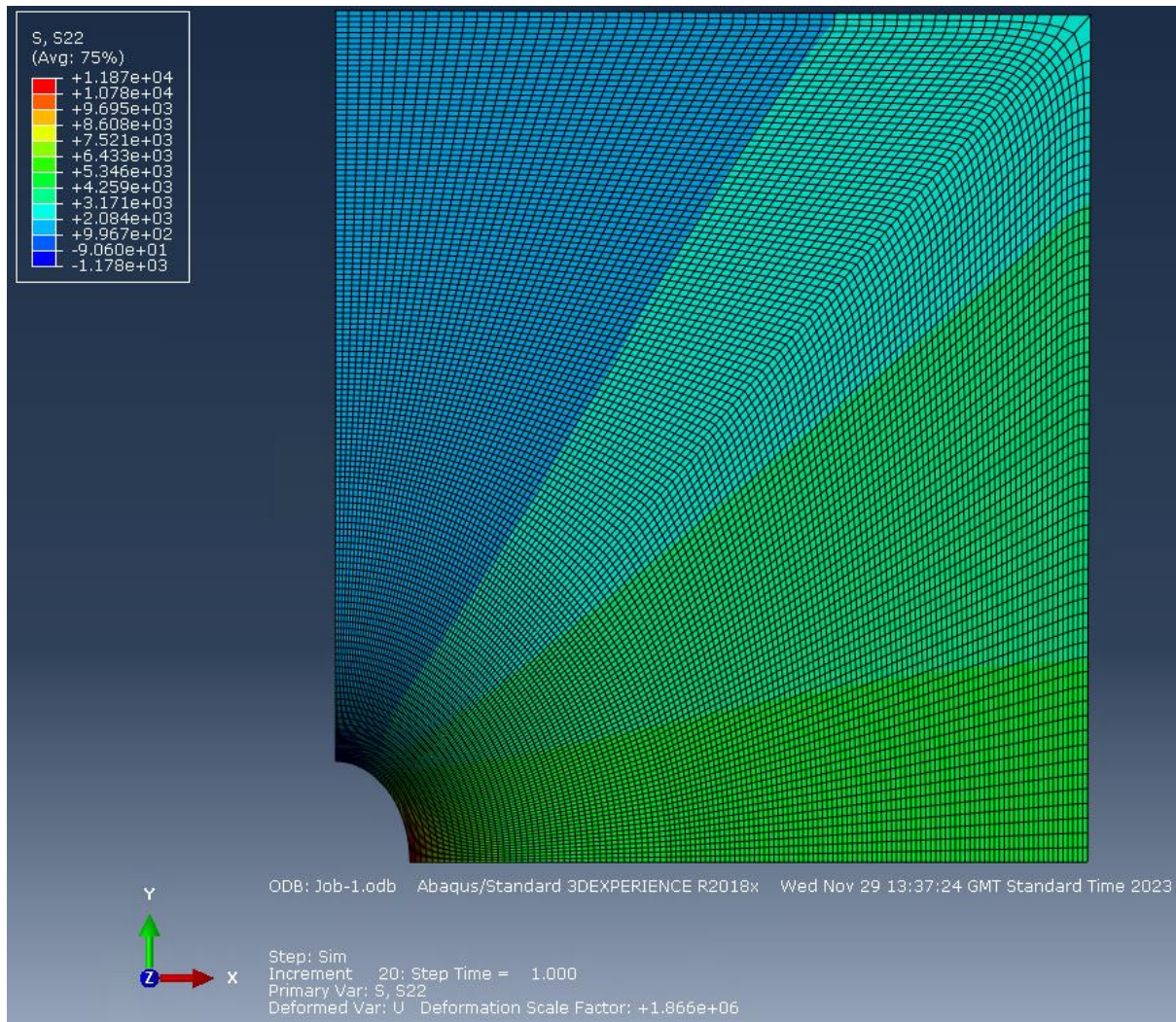


Figure 22: FEA of S22 along arc length

S12

```

dataTable = S12Hole;
columnHeaders = {'X','S12Hole'};
columnA = dataTable.(columnHeaders{1});
columnB = dataTable.(columnHeaders{2});
sigma_1 = 4500;
sigma_2 = 1000;
a = 0.1;
c = columnA; % Arc length of 0 to pi
plot(c,columnB ./ (sigma_1));

title('SCF along Arc Length');
xlabel('Arc Length');
ylabel('SCF');
grid on

```

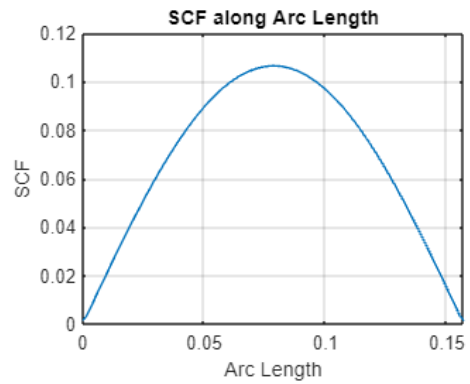


Figure 23: S12 along arc length

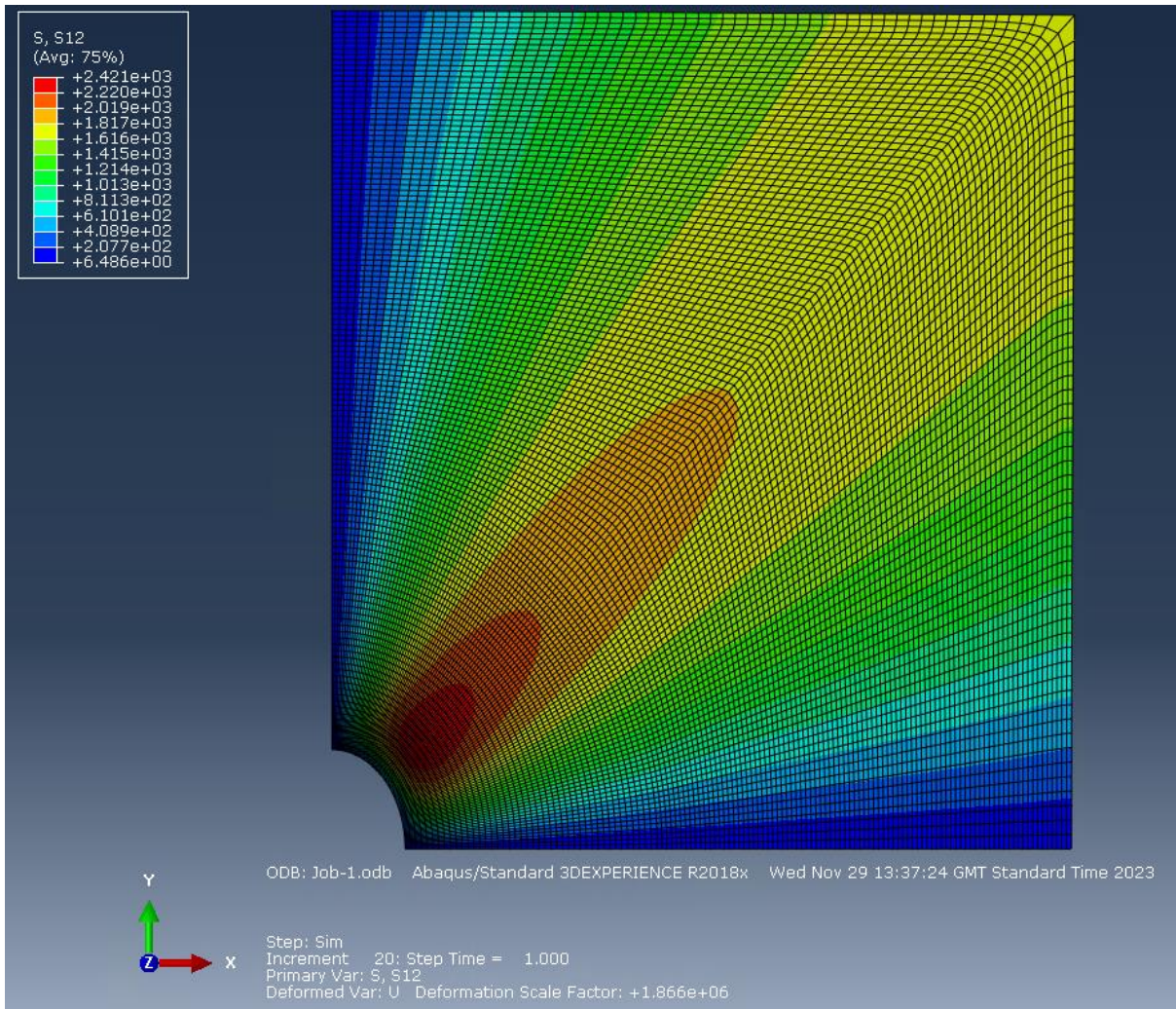


Figure 24: FEA of S12 along arc length

From figures 19-24, the largest SCF is  $\sigma_{\theta\theta}$  at  $\theta = 0$ , which is  $S = 2.63773$ .

### Reasons for Discrepancies

Thickness is assumed to be 0 in theoretical calculation, but its set at 1 in ABAQUS.

Mesh density is finite in ABAQUS, the finer the mesh, the closer it gets to 2.78.

Assuming plate dimension is infinite, length and width is much larger than radius of the hole.

### 3.2 Effect of Plate Dimension on Stress Concentration Factor

The simulation was done again with a different width and thickness to see its effect on the stress concentration factor (SCF).

Simulation Width	$\frac{d}{W}$	Thickness	SCF
1	0.1	1	2.63773
2	0.05	1	2.58667
1	0.1	0.5	2.76737

Table 2: Parameters' effects on SCF

Table 2 shows the effect of the plate width and thickness on SCF.

$\frac{d}{W}$  represents the ratio between the hole diameter and the plate width, which is assumed to be 0 in the theoretical calculation for SCF. This is when the dimension of the plate approaches infinity.

The findings from table 2 show that when finite plate dimensions are considered, SCF is lower than the theoretical value of 2.78. The higher  $\frac{d}{W}$  gets, the closer it approaches the theoretical SCF of 2.78. Similarly, as the thickness approaches 0, the theoretical SCF of 2.78 is approached.

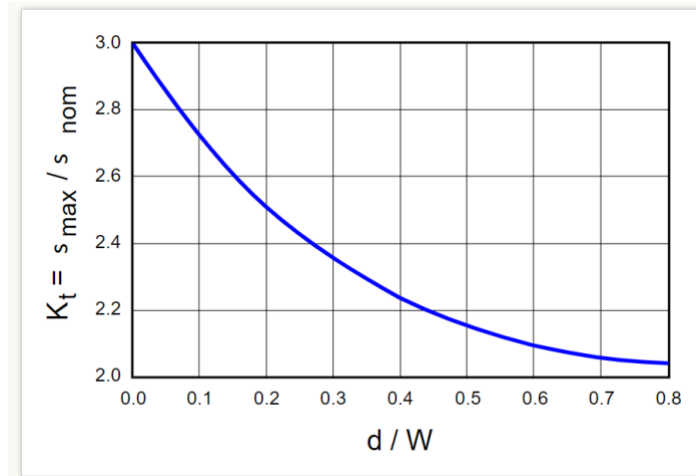


Figure 25: Relationship between SCF and  $d/W$

Kirsch [4] derived the relationship between  $\frac{d}{W}$  and SCF, represented as shown in figure 25. As  $\frac{d}{W}$  approaches 1, SCF decreases. This validates the trend found from table 2.

Vaz and Yang [5] [6] investigated the variation of SCF through the thickness for isotropic plates under a tensile stress. It is discovered that a smaller thickness results to a larger SCF, which is consistent with the results from table 2.

## References

- [1] classes.engineering.wustl.edu. (n.d.). Getting Started with ABAQUS/Explicit: Keywords Version (v6.6). [online] Available at: <https://classes.engineering.wustl.edu/2009/spring/mase5513/abaqus/docs/v6.6/books/gsx/default.htm?startat=ch04s01.html>.
- [2] docs.software.vt.edu. (n.d.). Selecting a meshing technique. [online] Available at: <https://docs.software.vt.edu/abaqusv2022/English/SIMACAECAERefMap/simacae-t-mgnattributestechique.htm#:~:text=Abaqus%2FCAE%20selects%20As%20is> [Accessed 30 Nov. 2023].
- [3] Wustl.edu. (2023). ABAQUS/CAE User's Manual (v6.5-1). [online] Available at: <https://classes.engineering.wustl.edu/2009/spring/mase5513/abaqus/docs/v6.5/books/usi/default.htm?startat=pt06ch40s09hlb01.html> [Accessed 30 Nov. 2023].
- [4] McGinty, B. (2019). Stress Concentrations at Holes. [online] Fracturemechanics.org. Available at: <https://www.fracturemechanics.org/hole.html>.
- [5] Vaz, M.A., Cyrino, J.C.R. and Silva, G.G. da (2013). Three-Dimensional Stress Concentration Factor in Finite Width Plates with a Circular Hole. World Journal of Mechanics, 03(03), pp.153–159. doi:<https://doi.org/10.4236/wjm.2013.33013>.
- [6] The concentration of stress and strain in finite thickness elastic plate containing a circular hole. (2008). International Journal of Solids and Structures, [online] 45(3-4), pp.713–731. doi:<https://doi.org/10.1016/j.ijsolstr.2007.08.030>.